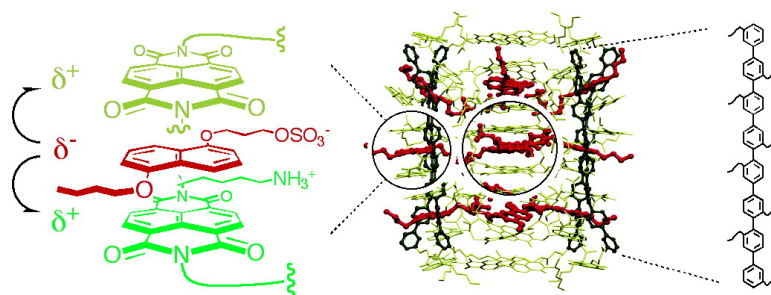


## Synthetic Ion Channels with Rigid-Rod $\pi$ -Stack Architecture that Open in Response to Charge-Transfer Complex Formation

Pinaki Talukdar, Guillaume Bollot, Jiri Mareda, Naomi Sakai, and Stefan Matile

*J. Am. Chem. Soc.*, **2005**, 127 (18), 6528-6529 • DOI: 10.1021/ja051260p • Publication Date (Web): 15 April 2005

Downloaded from <http://pubs.acs.org> on March 25, 2009



### More About This Article

Additional resources and features associated with this article are available within the HTML version:

- Supporting Information
- Links to the 9 articles that cite this article, as of the time of this article download
- Access to high resolution figures
- Links to articles and content related to this article
- Copyright permission to reproduce figures and/or text from this article

[View the Full Text HTML](#)

## Synthetic Ion Channels with Rigid-Rod $\pi$ -Stack Architecture that Open in Response to Charge-Transfer Complex Formation

Pinaki Talukdar, Guillaume Bollot, Jiri Mareda, Naomi Sakai, and Stefan Matile\*

Department of Organic Chemistry, University of Geneva, Geneva, Switzerland

Received February 28, 2005; E-mail: stefan.matile@chiorg.unige.ch

In this report, we introduce aromatic electron donor–acceptor interactions to construct synthetic ion channels that open in response to chemical stimulation. The creation of synthetic ion channels and pores from scaffolds that are not known to occur in nature is a topic of increasing scientific concern.<sup>1–15</sup> Since some years, scientific attention is steadily shifting from unifunctional channels<sup>8</sup> and pores toward “smart” supramolecular architecture that recognizes nontrivial ions<sup>9</sup> or specific characteristics of lipid bilayer membranes, such as membrane potential,<sup>10</sup> surface potential, membrane composition, and stress.<sup>1</sup> Synthetic multifunctional pores<sup>2</sup> were introduced<sup>11</sup> to combine molecular translocation with molecular recognition<sup>11</sup> and transformation<sup>12</sup> for practical applications, such as the detection of chemical reactions.<sup>13</sup> Current research on the use of not only synthetic<sup>1,2</sup> but also bioengineered<sup>16,17</sup> and biological<sup>18</sup> ion channels and pores as sensors focuses, however, almost<sup>14</sup> exclusively on blockage. Herein, the plum-colored charge-transfer complexes formed by dialkoxynaphthalene (DAN) donors and naphthalenediimide (NDI) acceptors, a classical motif in supramolecular chemistry,<sup>19–22</sup> are introduced to create synthetic ion channels with a novel rigid-rod  $\pi$ -stack architecture that open rather than close in response to guest binding.

We felt that this conceptually new approach could provide access to ligand gating for the following reasons (Figure 1). Self-assembly of octakis(NDI)-*p*-octiphenyls **1** was expected to yield  $\pi$ -helices **1<sup>HH</sup>** rather than  $\pi$ -barrels **1<sup>n</sup>** because of the mismatched repeat distances of stacked NDI hoops and rigid-rod *p*-octiphenyl staves. Upon intercalation of DAN ligands **2** into their mismatched NDI stacks, these closed ion channels **1<sup>HH</sup>** were expected to undergo a conformational change by a cooperative untwisting<sup>23</sup> to give open

ion channels **1<sup>n</sup>·2<sup>m</sup>**. Previously established design strategies were applied in addition to promote cylindrical self-assembly into supramolecular oligomers rather than linear self-assembly into supramolecular polymers (nonplanar rigid-rod staves),<sup>2</sup> to access hollow higher oligomers rather than closed dimers (internal crowding<sup>24</sup> and internal charge repulsion;<sup>2</sup> Figure 1A, blue), and to orient  $\pi$ -stacks<sup>25</sup> (hydrogen-bonded chains between flanking amides; Figure 1A and D, red). Geometry-minimized models **1<sup>n</sup>·2<sup>m</sup>** were in good agreement with these expectations. The hydrogen-bonded chains lining the  $\pi$ -stacks (Figure 1D, red arrows), for example, were not disrupted by ligand intercalation.

Target molecules **1** and **2** were synthesized from commercial starting materials in overall 13 and 2 steps, respectively (Figures 1 and 2). The NDI hoops were prepared by reacting amines **3** and **4** with dianhydride **5** followed by *Z*-deprotection of the obtained NDI **6** (Scheme 1). Coupling of the resulting amines **7** with the carboxylic acids lining the scaffold of the previously reported<sup>12</sup> *p*-octiphenyl **8** followed by hoop deprotection with TFA gave target molecule **1**. Structure and sample homogeneity were confirmed by NMR spectroscopy, ESI mass spectrometry, and reverse-phase HPLC.

Ligand gating was probed in EYPC-LUVs $\Delta$ HPTS (i.e., large unilamellar vesicles composed of egg yolk phosphatidylcholine and loaded with the pH-sensitive dye, 8-hydroxy-1,3,6-pyrenetrisulfonate). In this assay, the ratiometric changes in HPTS emission are used to follow the collapse of an applied pH gradient by either H<sup>+</sup>/M<sup>+</sup> or OH<sup>-</sup>/A<sup>-</sup> antiport.<sup>26,27</sup> As anticipated, neither rod **1** nor ligand **2** were highly active (Figure 2Ad and Ae). Once mixed together, however, they were active (Figure 2Aa). Dose response

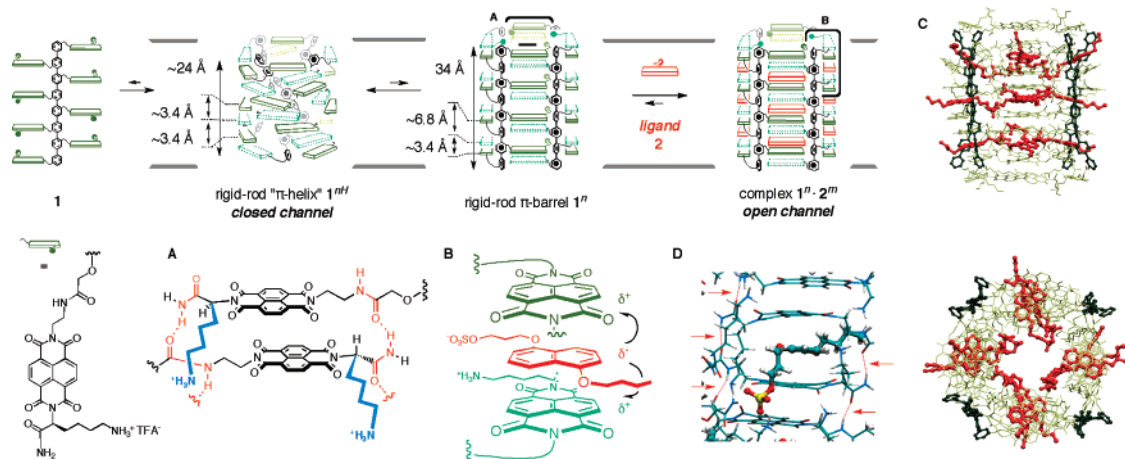


**Figure 1.** Ligand-gated opening of notional rigid-rod  $\pi$ -helix **1<sup>HH</sup>** into ion channel **1<sup>n</sup>·2<sup>m</sup>** by intercalation of DAN ligands **2** (red) into the mismatched NDI hoops of transient  $\pi$ -barrel **1<sup>n</sup>** with magnified views of (A) NDI–NDI stack highlighting internal crowding (blue) and H-bonded chains (red), and (B) DAN–NDI CT complex. (C) Geometry-optimized model of **1<sup>n</sup>·2<sup>m</sup>**,  $n = 4$ ,  $m = 12$ , in side (top) and axial view (bottom); *p*-octiphenyls (dark green) and DANs (red) are in ball-and-stick model, NDIs (light green) in wires, 50% amine protonation, 0% sulfate protonation, H omitted. (D) Detail of a minimized model of **1<sup>n</sup>·2<sup>m</sup>** with H-bonded chains (red, arrows, C cyan, H gray, N blue, O red, S yellow). All shown suprastructures are, in part, speculative simplifications that are, however, consistent with experimental data (Figure 2)<sup>23,24,28</sup> and molecular models (C and D); stoichiometries of supramolecules are unknown.

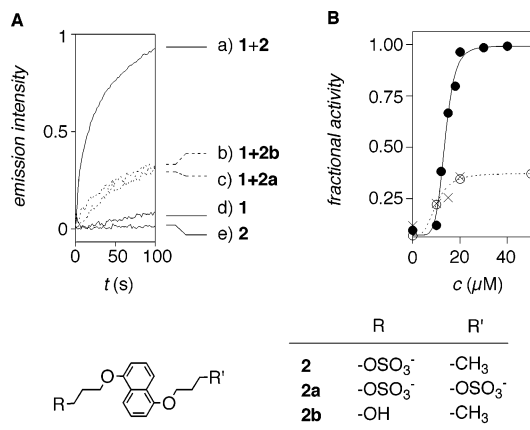
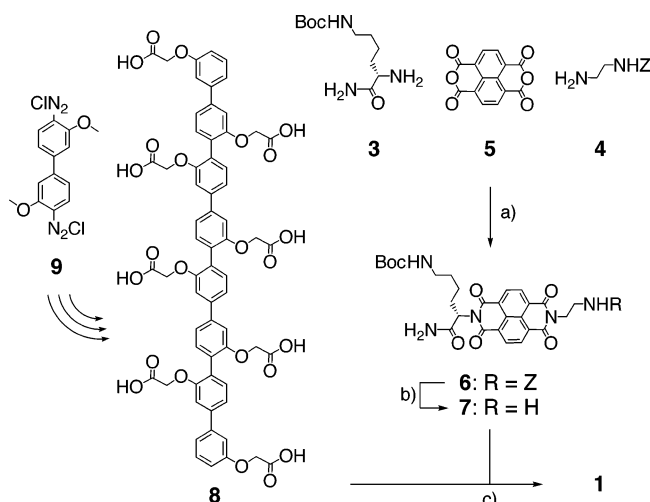


**Figure 2.** Changes in activity of NDI rod **1** (1a: Ad) in response to (D) DAN ligands **2**, **2a** (Ac, B○) and **2b** (Ab, B×). (A) Fractional HPTS emission,  $I$  ( $\lambda_{\text{ex}} = 450 \text{ nm}$ ,  $\lambda_{\text{em}} = 510 \text{ nm}$ ), as a function of time during addition of base ( $\Delta\text{pH} = 0.9$ ) followed by **2** (a and e,  $20 \mu\text{M}$ ), **2a** (c,  $40 \mu\text{M}$ ), or **2b** (b,  $15 \mu\text{M}$ ), and then **1** (a–d,  $1.6 \mu\text{M}$ ,  $t = 0 \text{ s}$ ) to EYPC-LUVs/HPTS (10 mM HEPES, 100 mM NaCl, pH 7.0). (B) Activity of **1** ( $1.6 \mu\text{M}$ ) as a function of the concentration of **2** (●), **2a** (○), and **2b** (×).

### Scheme 1<sup>a</sup>



<sup>a</sup> (a) TEA, DMF, 48 h,  $40^\circ\text{C}$ , 50%; (b)  $\text{H}_2$ , Pd(OH)<sub>2</sub>/C, MeOH, 6 h, rt, 91%; (c) 1. HATU, DMF, 2,6-di-*tert*-butylpyridine, 24 h, rt, 59%, 2. TFA/CH<sub>2</sub>Cl<sub>2</sub> 1:1, 73% (for **9** → **8** in 9 steps; see ref 12).

to **2** revealed an effective concentration  $\text{EC}_{50} = 13.7 \mu\text{M}$  and a Hill coefficient  $n = 6.5$  (Figure 2B (●)). The latter value was high, characterizing the notional supramolecule **1<sup>nH</sup>** as a sponge that swallows at least<sup>23</sup> six ligands **2** to form the open ion channel **1<sup>n\*2<sup>m</sup></sup>**. The much weaker but clearly synergistic effect observed with **1** and DAN control **2b** without sulfate showed significant contributions of aromatic interactions as well as internal ion pairing for ligand gating (Figure 2Ab/B(×)). Similar loss of relevant activity without hydrophobic tail in DAN control **2a** confirmed the importance of external hydrophobicity of barrel-stave supramolecule **1<sup>n\*2<sup>m</sup></sup>** for ligand gating (Figure 2Ac/B(○)). Other intercalators, such as AMP or GMP, were inactive.

The selectivity of ion channel **1<sup>n\*2<sup>m</sup></sup>** was consistent with the designed, confined, and cationic interior. For example, organic ions such as 8-aminonaphthalene-1,3,6-trisulfonate anions or *p*-xylene bispyridinium cations were not transported, as expected from the internal diameter in molecular models (Figure 1C,  $d = 5.4 \text{ \AA}$ ).<sup>28</sup> Competitive inhibition of OH<sup>-</sup> influx by external anions implied an OH<sup>-</sup>/A<sup>-</sup> antiport mechanism with inhibition sequence<sup>29,27</sup> SO<sub>4</sub><sup>2-</sup> > NO<sub>3</sub><sup>-</sup> ≈ I<sup>-</sup> > Cl<sup>-</sup> ≈ Br<sup>-</sup> > AcO<sup>-</sup> > F<sup>-</sup>. Cations such as Na<sup>+</sup>,

K<sup>+</sup>, Rb<sup>+</sup>, or Cs<sup>+</sup> did not interfere with OH<sup>-</sup>/A<sup>-</sup> exchange. The appearance of the typical plum color of charge-transfer complexes completed this consistent experimental evidence for rationally designed, highly cooperative ligand gating of synthetic anion channels by aromatic electron donor–acceptor interactions. Taken together, these findings<sup>23,24,28</sup> confirmed the potential of the new rigid-rod  $\pi$ -stack architecture to expand the practical usefulness of synthetic multifunctional ion channels and pores<sup>13</sup> toward electron-transfer processes.

**Acknowledgment.** We thank M. R. Shah for assistance in synthesis, D. Jeannerat, A. Pinto, and J.-P. Saulnier for NMR measurements, P. Perrottet and the group of F. Gülaçar for MS measurements, H. Eder for elemental analyses, and the Swiss NSF for financial support (including National Research Program “Supramolecular Functional Materials” 4047-057496).

**Supporting Information Available:** Experimental part (8 pages, print/PDF). This material is available free of charge via the Internet at <http://pubs.acs.org>.

### References

- Matile, S.; Som, A.; Sordé, N. *Tetrahedron* **2004**, *60*, 6405–6435.
- Sakai, N.; Mareda, J.; Matile, S. *Acc. Chem. Res.* **2005**, *38*, 79–87.
- Hector, R. S.; Gin, M. S. *Supramol. Chem.* **2005**, *17*, 129–134.
- Mitchell, K. D. D.; Fyles, T. M. In *Encyclopedia of Supramolecular Chemistry*; Atwood, J. L., Steed, J. W., Eds.; Marcel Dekker: New York, 2004; pp 742–746.
- Koert, U. Synthetic Ion Channels. *Bioorg. Med. Chem.* **2004**, *12*, 1277–1350.
- Boon, J. M.; Smith, B. D. *Curr. Opin. Chem. Biol.* **2002**, *6*, 749–756.
- Gokel, G. W.; Mukhopadhyay, A. *Chem. Soc. Rev.* **2001**, *30*, 274–286.
- Tabushi, I.; Kuroda, Y.; Yokota, K. *Tetrahedron Lett.* **1982**, *23*, 4601–4604.
- Tanaka, Y.; Kobuke, Y.; Sokabe, M. *Angew. Chem., Int. Ed. Engl.* **1995**, *34*, 693–694.
- Fyles, T. M.; Loock, D.; Zhou, X. *J. Am. Chem. Soc.* **1998**, *120*, 2997–3003.
- Sakai, N.; Baumeister, B.; Matile, S. *ChemBioChem* **2000**, *1*, 123–125.
- Baumeister, B.; Sakai, N.; Matile, S. *Org. Lett.* **2001**, *3*, 4229–4232.
- Das, G.; Talukdar, P.; Matile, S. *Science* **2002**, *298*, 1600–1602.
- Gorteau, V.; Perret, F.; Bollot, G.; Mareda, J.; Lazar, A. N.; Coleman, A. W.; Tran, D.-H.; Sakai, N.; Matile, S. *J. Am. Chem. Soc.* **2004**, *126*, 13592–13593.
- Jeon, Y. J.; Kim, H.; Jon, S.; Selvapalam, N.; Oh, D. H.; Seo, I.; Park, C.-S.; Jung, S. R.; Koh, D.-S.; Kim, K. *J. Am. Chem. Soc.* **2004**, *126*, 15944–15945.
- Bayley, H.; Cremer, P. S. *Nature* **2001**, *413*, 226–230.
- Terrettz, S.; Ulrich, W.-P.; Guerrini, R.; Verdini, A.; Vogel, H. *Angew. Chem., Int. Ed.* **2001**, *40*, 1740–1743.
- Deamer, D. W.; Branton, D. *Acc. Chem. Res.* **2002**, *35*, 817–825.
- Lokey, R. S.; Iverson, B. L. *Nature* **1995**, *375*, 303–305.
- Gabriel, G. J.; Iverson, B. L. *J. Am. Chem. Soc.* **2002**, *124*, 15174–15175.
- Furlan, R. L.; Otto, S.; Sanders, J. K. M. *Proc. Natl. Acad. Sci. U.S.A.* **2002**, *99*, 4801–4804.
- Vignon, S. A.; Jarrosson, T.; Iijima, T.; Tseng, H.-R.; Sanders, J. K. M.; Stoddart, J. F. *J. Am. Chem. Soc.* **2004**, *126*, 9884–9885.
- Changes in the circular dichroism (CD) spectrum of **1<sup>24</sup>** and the excimer emission of **2** during ligand gating were in support of (a) the helix-barrel transition from *M*-helix **1<sup>nH</sup>** to barrel **1<sup>n\*2<sup>m</sup></sup>**, and (b) the partitioning of **2** as dimers or oligomers into the lipid bilayer membrane before binding to **1** (for the influence of self-assembly on Hill coefficients, please see: Litvinchuk, S.; Bollot, G.; Mareda, J.; Som, A.; Ronan, D.; Shah, M. R.; Perrottet, P.; Sakai, N.; Matile, S. *J. Am. Chem. Soc.* **2004**, *126*, 10067–10075).
- Control experiments revealed that internally decrowded analogues of **1** (a) do not form ligand-gated ion channels and (b) are CD silent.
- Zhang, W.; Horoszewski, D.; Decatur, J.; Nuckolls, C. *J. Am. Chem. Soc.* **2003**, *125*, 4870–4873.
- Weiss, L. A.; Sakai, N.; Ghebremariam, B.; Ni, C.; Matile, S. *J. Am. Chem. Soc.* **1997**, *119*, 12142–12149.
- Tedesco, M. M.; Ghebremariam, B.; Sakai, N.; Matile, S. *Angew. Chem., Int. Ed.* **1999**, *38*, 540–543.
- Single- and multichannel conductance experiments in planar EYPC bilayers were in agreement with the ligand-gated formation of anion selective, long-lived ion channels **1<sup>n\*2<sup>m</sup></sup>** with an inner diameter compatible with above size-exclusion experiments in EYPC vesicles and molecular models. The material referred to in refs 23, 24, and 28 will be published as a full paper.
- Wright, E. M.; Diamond, J. M. *Physiol. Rev.* **1977**, *57*, 109–156.

JA051260P